Inorganic Chemistry

pubs.acs.org/IC

Communication

Metal–Organic Nanocapsules with Functionalized s-Heptazine Ligands

Lindley Maxwell, Héctor Martínez, Alejandro Martín-Rodríguez, Silvia Gómez-Coca, Kari Rissanen,* and Eliseo Ruiz*

Cite This: *Inorg. Chem.* 2021, 60, 570–573

Read Online

ABSTRACT: A metalloorganic capsule was synthesized where the ligand is a derivative of heptazine with three carboxylic groups that are coordinated to Cu^{II} cations, forming paddle-wheel motifs. Each nanocapsule is neutral, with 12 Cu^{II} centers and 8 ligands adopting a rhombicuboctahedron shape. It has almost 3 nm diameter, and the main intermolecular interactions in the solid are $\pi\cdots\pi$ stacking between the C_6N_7 heptazine moieties. The nanocapsules can form monolayers deposited on graphite as observed by atomic force microscopy, which confirms their stability in solution.

Studies of the rational synthesis of discrete metal–organic nanocapsules with specific shapes and structures have been extensively carried out by several research groups.[1−14] An additional feature of the self-assembly process in the synthetic process is to provide these nanocapsules with additional chemical and physical properties. In this case, we have employed as the ligand a heptazine derivative synthesized from polymeric derivatives of s-heptazine,[15] also known as graphitic carbon nitride (g-C_3N_4), which has been recently proposed for many catalytic processes (Figure 1).[16−19] One of the main problems in working with heptazine derivatives is their low solubility. The goal of this manuscript is to show that it is possible to overcome the solubility problems and synthesize nanocapsules with the C_6N_7 moieties. In addition, this approach shows that the larger size of the heptazine ligands opens the possibility of generating nanocapsules while the equivalent s-triazine system (Figure 1) results in periodic metal–organic frameworks (Figure S6).[20]

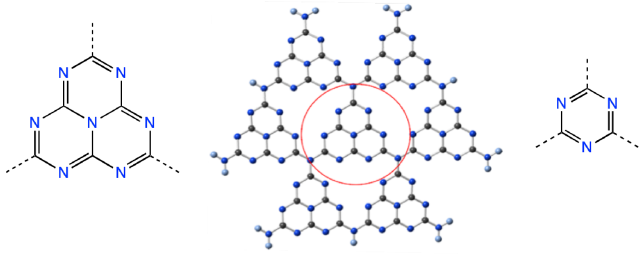

Figure 1. (left) s-Heptazine, (center) g-C_3N_4, and (right) s-triazine.

The goal was to form a nanocapsule using a 4-connected paddle-wheel subunit $[M_2(-COO)_4]$ as the vertex, where the carboxylic binding groups belong to a tritopic heptazine derivative ligand. The synthesis of this ligand involves several steps [see Figure 2 and the Supporting Information (SI) for reaction details].[21] The first step is pyrolysis of urea at high temperature to obtain the polymeric $[C_6N_7(NH)(NH_2)]_n$ *melon* **1**; depending of the thermal treatment, we can also reach the dehydrogenated system g-C_3N_4. The second step is alkali hydrolysis to synthesize the trialkoxide derivative **2** through a solid-state reaction with PCl_5 to obtain the trichloro derivative cyameluric chloride (**3**). Finally, the substitution reaction with 4-piperidinecarboxylic acid (4pac, also called isonipecotic acid) results in the ligand 1,1′,1″-(1,3,3a^1,4,6,7,9-heptaazaphenalene-2,5,8-triyl)tris(piperidine-4-carboxylic acid) (**4** or h3tp4c). It is a microwave-assisted reaction that uses $NaHCO_3$ as the base and 1,4-dioxane as the solvent.

The relative low solubility of **4** makes reaction with the metal difficult (see Table S1 for the results of multiple attempts, also including cases with Zn^{II} cations), but reaction with $Cu(NO_3)_2\cdot 3H_2O$ in dimethyl sulfoxide (DMSO) in a sealed vial at 110 °C results in the Cu_{12} nanocapsule **5** (Figure 3). A similar reaction with an equivalent triazine ligand and Zn^{II} cations results in a periodic structure[20] with a metal/ligand ratio of 12:4. In that case, on each paddle-wheel structure, two of the carboxylic acid group ligands are coordinated to the same moiety, but the other two are coordinated to a different unit (Figure S6). However, the relatively large size of the heptazine derivative ligand allows one to form a nanocapsule with 12 Cu^{II} cations and 8 heptazine ligands, resulting in a neutral system. The structure of **5** can be described as a rhombicuboctahedron (Figure S6), where the six Cu_2 paddle-wheel subunits (including the piperidine moiety) form the six edges of the cube and the heptazine moieties constitute the eight triangular faces.

The charge-neutral nanocapsule **5** packs (Figures 4, bottom, and S7) through $\pi-\pi$ interactions with an interplanar distance

Received: December 11, 2020
Published: December 23, 2020

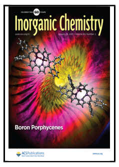

https://dx.doi.org/10.1021/acs.inorgchem.0c03631

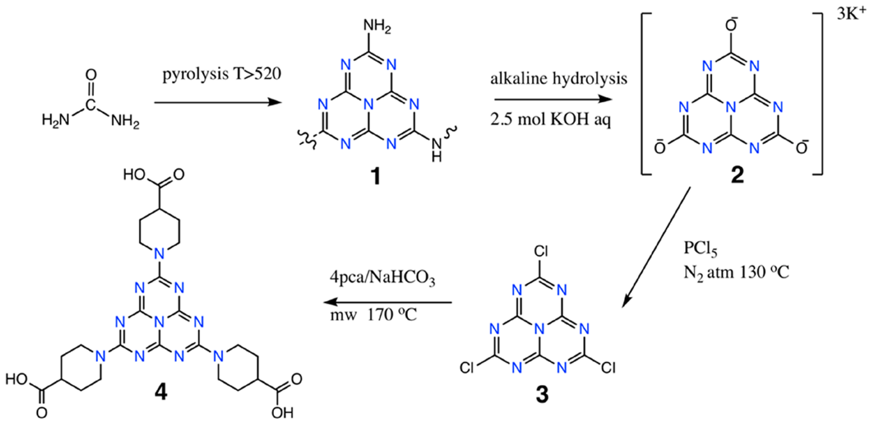

Figure 2. Synthesis of the ligand 4 (mw = microwave; see SI for characterization).

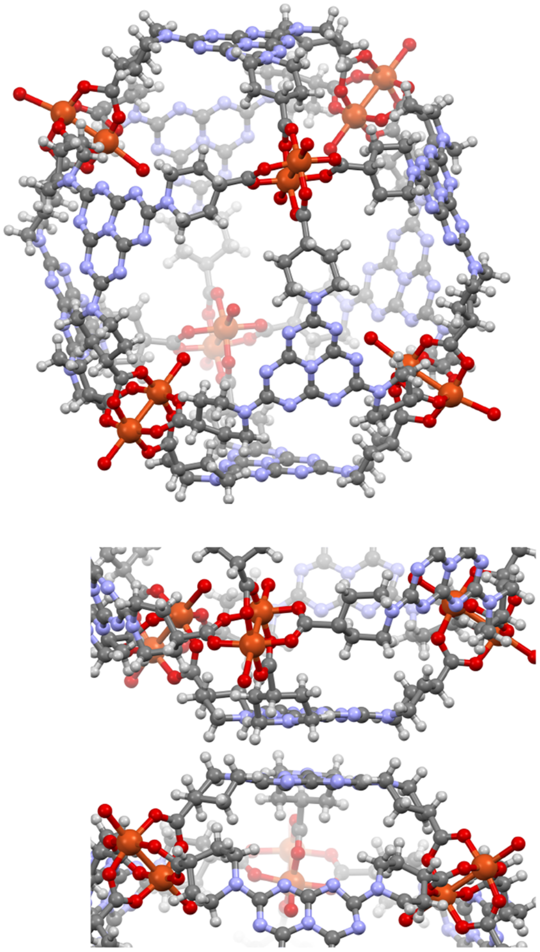

Figure 3. (above) Structure of complex **5** [$Cu_{12}(tp4c)_8(H_2O)_{12}$]. Orange, blue, gray, and red ellipsoids correspond to Cu, N, C, and O atoms, respectively. (below) Structure details of the intermolecular $\pi-\pi$ stacking through the heptazine groups between two neighboring Cu_{12} nanocapsules.

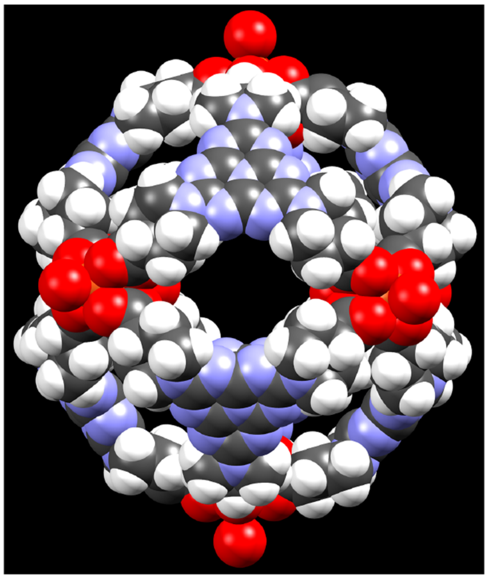

Figure 4. Space-filling model presentation of the structure of complex **5** [$Cu_{12}(tp4c)_8(H_2O)_{12}$ showing the shape of the 0.7 nm windows.

of 3.5 Å between the C_6N_7 heptazine units of the nanocapsules. The diameter of the nanocapsule is ca. 3 nm with a 2.5 nm distance between the outer paddle-wheel Cu atoms. The nanocapsule has an internal cavity of 2600 Å^3 (see cavity details in Figure S8), but because of the moderate resolution of the diffraction data, none of the DMSO solvent molecules could be located inside the cavity. The nanocapsule is not completely closed because there are 10 ellipsoidal windows, ca. 0.7 nm in diameter, allowing the small solvent molecules to "swim" through the cavity in the solution.

In order to complete the structural characterization, we have employed a 1:100 dilution of the mother liquor to deposit a monolayer of the complex **5** on highly oriented pyrolytic graphite (immersion time 30 s). The sample was abundantly cleaned with DMSO in order to eliminate the molecules that were not attached to the substrate through $\pi-\pi$ interactions. The sample was measured using atomic force microscopy (AFM; see details in the SI, section 5). We performed a scratch with the microscope tip of the monolayer to determine the thickness of the monolayer (Figure 5), cleaning the substrate surface. The thickness value around 2.2 nm is in agreement with the size of the molecule (the molecule is slightly larger, almost 3 nm in the direction of the two outer paddle-wheel groups), assuming that one of the heptazine groups is interacting with the graphite surface. This fact confirms the stability of complex **5** in solution despite its large size.

The photochemical properties of ligand **4** (Figures 6 and S9) and the dodecanuclear complex **5** (Figure S10) have been explored. From these data, we can outline some points: (i) The heptazine-based ligand **4** has a high absorbance with an

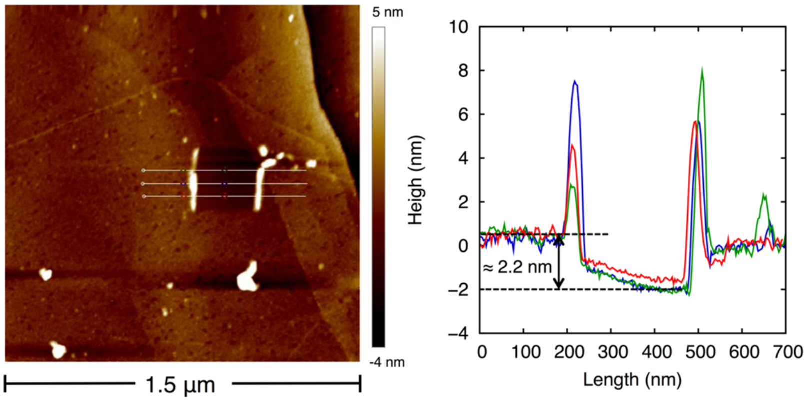

Figure 5. (left) AFM image of the monolayer of **5** deposited on highly oriented pyrolytic graphite. (right) Cross-sectional profiles in the tip-scratched area at the position indicated by the lines in the AFM image.

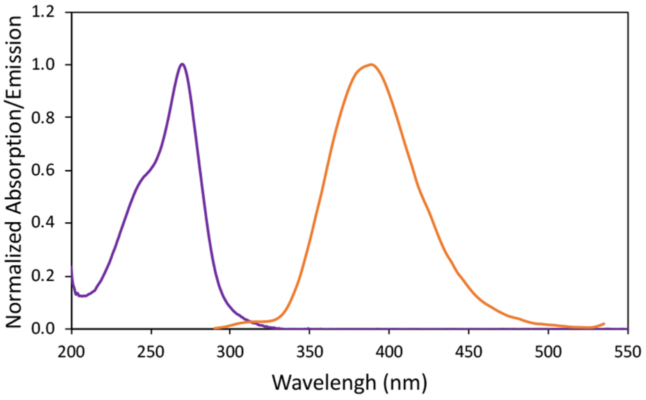

Figure 6. Absorption (purple) and emission (orange) spectra of ligand **4** at 10^{-6} M (Figure S9 at different concentrations in methanol). The excitation wavelength is 273 nm.

extinction coefficient of 1.1×10^5 M^{-1} cm^{-1}, while the value for the complex is 1 order of magnitude smaller, 1.8×10^4 M^{-1} cm^{-1}. (ii) Ligand **4** has a large Stokes shift of 110 nm (absorption 273 nm and emission 383 nm; Figure 5), indicating a large structural rearrangement of the molecule in the excited state. These structural variations should lead to a new conformation in the lower-energy excited state that might be responsible for the red shift in the emission maxima. The quantum yield of ligand **4** determined by using an integrating sphere is 3.8%. (ii) The quenching effects in $[Cu_{12}(tp4c)_8(H_2O)_{12}]$ are important, and the system does not present fluorescence (see the UV−vis spectra; Figure S10). It is worth noting that a previously reported Cu_3 complex[21] with pyridylheptazine ligands shows fluorescence because the Cu^{II} $d_{x^2-y^2}$ orbitals are orthogonal to the π system of the heptazine moieties; however, that is not the case in **5** (see ligand orbitals in Figure S11 and the relative position of the heptazine and paddle-wheel groups in Figure S5).

Finally, we explored the host⋯guest features of the nanocapsule **5** by replacing the solvent DMSO molecules. A filtered and cleaned sample was introduced in *N*,*N*-dimethylformamide (DMF) over 1 week. The results for the IR spectra are represented in Figure 7. The DMSO characteristic peaks (blue curve) at 3000 and 1025 cm^{-1} decrease or disappear in the DMF sample (green curve; new DMF characteristic peaks at 2930 and 1093 cm^{-1}). Thus, we can conclude that there is a replacement of the DMSO by the DMF host molecules.

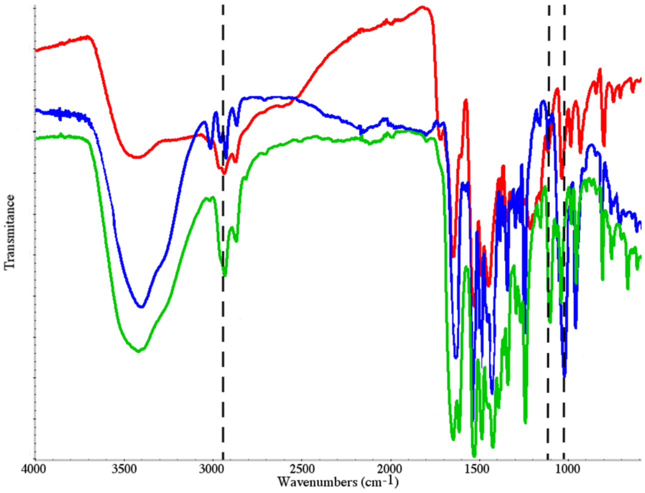

Figure 7. IR spectra (recorded with attenuated total reflectance) for ligand **4** (red) provided as a reference and nanocapsule **5** with DMSO and DMF (blue and green, respectively). Dashed lines are included to mark the key differences.

In summary, relatively large metal−organic nanocapsules can be self-assembled by using carboxylic−heptazine ligands. AFM experiments show the stability of the nanocapsules in solution. The presence of the C_6N_7 heptazine moiety in the ligand opens wide possibilities of combining its photochemical, host⋯guest, and catalytic properties with those of the metals. Furthermore, this is an example of how to circumvent the problems to synthesize complex systems with low-solubility ligands.

■ ASSOCIATED CONTENT

Supporting Information

The Supporting Information is available free of charge at https://pubs.acs.org/doi/10.1021/acs.inorgchem.0c03631.

Details of synthesis and characterization (IR data, NMR, mass spectrometry, AFM), DFT calculations, and crystallographic data (PDF)

Accession Codes

CCDC 1951192 contains the supplementary crystallographic data for this paper. These data can be obtained free of charge via www.ccdc.cam.ac.uk/data_request/cif, or by emailing data_request@ccdc.cam.ac.uk, or by contacting The Cambridge Crystallographic Data Centre, 12 Union Road, Cambridge CB2 1EZ, UK; fax: +44 1223 336033.

AUTHOR INFORMATION

Corresponding Authors

Kari Rissanen − *Nanoscience Center, Department of Chemistry, University of Jyvaskyla, 40014 Jyväskylä, Finland;* orcid.org/0000-0002-7282-8419; Email: kari.t.rissanen@jyu.fi

Eliseo Ruiz − *Departament de Química Inorgànica and Institut de Recerca de Química Teòrica i Computacional, Universitat de Barcelona, 08028 Barcelona, Spain;* orcid.org/0000-0001-9097-8499; Email: eliseo.ruiz@qi.ub.edu

Authors

Lindley Maxwell − *Departament de Química Inorgànica and Institut de Recerca de Química Teòrica i Computacional, Universitat de Barcelona, 08028 Barcelona, Spain*

Héctor Martínez − *Departament de Química Inorgànica and Institut de Recerca de Química Teòrica i Computacional, Universitat de Barcelona, 08028 Barcelona, Spain*

Alejandro Martín-Rodríguez − *Departament de Química Inorgànica and Institut de Recerca de Química Teòrica i Computacional, Universitat de Barcelona, 08028 Barcelona, Spain*

Silvia Gómez-Coca − *Departament de Química Inorgànica and Institut de Recerca de Química Teòrica i Computacional, Universitat de Barcelona, 08028 Barcelona, Spain;* orcid.org/0000-0002-2299-4697

Complete contact information is available at: https://pubs.acs.org/10.1021/acs.inorgchem.0c03631

Notes

The authors declare no competing financial interest.

ACKNOWLEDGMENTS

This work had financial support by the Ministerio de Ciencia e Innovación through Grants PGC2018-093863-B-C21 and MDM-2017-0767 and by the Generalitat de Catalunya through Grant SGR2017-1289. E.R. thanks the Generalitat de Catalunya for his ICREA Academia grant. L.M. thanks Conicyt-Chile for a predoctoral fellowship. S.G.-C. thanks the Generalitat de Catalunya for a Beatriu de Pinós Fellowship (2017 BP 00080). We thank the CSUC for computational resources. Characterization of the samples was carried out in the Centres Científics i Tecnològics de la Universitat de Barcelona.

REFERENCES

(1) Kaphan, D. M.; Levin, M. D.; Bergman, R. G.; Raymond, K. N.; Toste, F. D. A supramolecular microenvironment strategy for transition metal catalysis. *Science* **2015**, *350*, 1235−1238.

(2) Dai, F.-R.; Sambasivam, U.; Hammerstrom, A. J.; Wang, Z. Synthetic Supercontainers Exhibit Distinct Solution versus Solid State Guest-Binding Behavior. *J. Am. Chem. Soc.* **2014**, *136*, 7480−7491.

(3) Cook, T. R.; Stang, P. J. Recent Developments in the Preparation and Chemistry of Metallacycles and Metallacages via Coordination. *Chem. Rev.* **2015**, *115*, 7001−7045.

(4) Caulder, D. L.; Raymond, K. N. Supermolecules by design. *Acc. Chem. Res.* **1999**, *32*, 975−982.

(5) Byrne, K.; Zubair, M.; Zhu, N.; Zhou, X.-P.; Fox, D. S.; Zhang, H.; Twamley, B.; Lennox, M. J.; Duren, T.; Schmitt, W. Ultra-large supramolecular coordination cages composed of endohedral Archimedean and Platonic bodies. *Nat. Commun.* **2017**, *8*, 15268.

(6) Brown, C. J.; Toste, F. D.; Bergman, R. G.; Raymond, K. N. Supramolecular Catalysis in Metal-Ligand Cluster Hosts. *Chem. Rev.* **2015**, *115*, 3012−3035.

(7) Pluth, M. D.; Raymond, K. N. Reversible guest exchange mechanisms in supramolecular host-guest assemblies. *Chem. Soc. Rev.* **2007**, *36*, 161−171.

(8) Pasquale, S.; Sattin, S.; Escudero-Adan, E. C.; Martinez-Belmonte, M.; de Mendoza, J. Giant regular polyhedra from calixarene carboxylates and uranyl. *Nat. Commun.* **2012**, *3*, 785.

(9) Zhang, D. W.; Ronson, T. K.; Nitschke, J. R. Functional Capsules via Subcomponent Self-Assembly. *Acc. Chem. Res.* **2018**, *51*, 2423−2436.

(10) Zarra, S.; Wood, D. M.; Roberts, D. A.; Nitschke, J. R. Molecular containers in complex chemical systems. *Chem. Soc. Rev.* **2015**, *44*, 419−432.

(11) Roberts, D. A.; Pilgrim, B. S.; Nitschke, J. R. Covalent post-assembly modification in metallosupramolecular chemistry. *Chem. Soc. Rev.* **2018**, *47*, 626−644.

(12) Wu, K.; Li, K.; Hou, Y.-J.; Pan, M.; Zhang, L.-Y.; Chen, L.; Su, C.-Y. Homochiral D4-symmetric metal-organic cages from stereogenic Ru(II) metalloligands for effective enantioseparation of atropisomeric molecules. *Nat. Commun.* **2016**, *7*, 10487.

(13) Yeung, C.-T.; Yim, K.-H.; Wong, H.-Y.; Pal, R.; Lo, W.-S.; Yan, S.-C.; Yee-Man Wong, M.; Yufit, D.; Smiles, D. E.; McCormick, L. J.; Teat, S. J.; Shuh, D. K.; Wong, W.-T.; Law, G.-L. Chiral transcription in self-assembled tetrahedral Eu4L6 chiral cages displaying sizable circularly polarized luminescence. *Nat. Commun.* **2017**, *8*, 1128.

(14) Zhang, T.; Zhou, L.-P.; Guo, X.-Q.; Cai, L.-X.; Sun, Q.-F. Adaptive self-assembly and induced-fit transformations of anion-binding metal-organic macrocycles. *Nat. Commun.* **2017**, *8*, 15898.

(15) Liebig, J. Ueber einige Stickstoff-Verbindungen. *Ann. Pharm.* **1834**, *10*, 1−47.

(16) Zhao, Z. W.; Sun, Y. J.; Dong, F. Graphitic carbon nitride based nanocomposites: a review. *Nanoscale* **2015**, *7*, 15−37.

(17) Wang, Y.; Wang, X. C.; Antonietti, M. Polymeric Graphitic Carbon Nitride as a Heterogeneous Organocatalyst: From Photochemistry to Multipurpose Catalysis to Sustainable Chemistry. *Angew. Chem., Int. Ed.* **2012**, *51*, 68−89.

(18) Ong, W. J.; Tan, L. L.; Ng, Y. H.; Yong, S. T.; Chai, S. P. Graphitic Carbon Nitride (g-C3N4)-Based Photocatalysts for Artificial Photosynthesis and Environmental Remediation: Are We a Step Closer To Achieving Sustainability? *Chem. Rev.* **2016**, *116*, 7159−7329.

(19) Cao, S. W.; Low, J. X.; Yu, J. G.; Jaroniec, M. Polymeric Photocatalysts Based on Graphitic Carbon Nitride. *Adv. Mater.* **2015**, *27*, 2150−2176.

(20) Zhao, X.; He, H.; Hu, T.; Dai, F.; Sun, D. Interpenetrating Polyhedral MOF with a Primitive Cubic Network Based on Supermolecular Building Blocks Constructed of a Semirigid C3-Symmetric Carboxylate Ligand. *Inorg. Chem.* **2009**, *48*, 8057−8059.

(21) Maxwell, L.; Gómez-Coca, S.; Weyhermüller, T.; Panyella, D.; Ruiz, E. A trinuclear CuII complex with functionalized s-heptazine N-ligands: molecular chemistry from a g-C3N4 fragment. *Dalton Trans* **2015**, *44*, 15761−15763.